Available online at www.sciencedirect.com

SciVerse ScienceDirect

Ceramics International 38 (2012) 5897–5905

CERAMICS INTERNATIONAL

www.elsevier.com/locate/ceramint

Influence of powder size on characteristics of air plasma sprayed silicon coatings

Yaran Niu [a,b,*], Xuebin Zheng [a,b,*], Xuanyong Liu [b], Heng Ji [a,b], Chuanxian Ding [a,b]

[a] Key Laboratory of Inorganic Coating Materials, Chinese Academy of Sciences, Shanghai, China
[b] Shanghai Institute of Ceramics, Chinese Academy of Sciences, Shanghai, China

Received 16 January 2012; received in revised form 21 March 2012; accepted 21 March 2012
Available online 21 April 2012

Abstract

Silicon powders with different medium sizes (114 μm, 79 μm and 31 μm, respectively) were used to fabricate coatings by air plasma spraying. The velocity and temperature of in-flight silicon particles during plasma spraying were determined. The composition and microstructure of the coatings were characterized and some physical properties of the coatings were measured. The obtained results showed that the size of silicon particles had great influence on their velocity and temperature in plasma flame. The oxidation of silicon particles in the spraying process was observed and is higher for particles of smaller sizes. Areas of silicon oxide in micrometer size are embedded and randomly distributed in the coating. The surface roughness and void content of silicon coatings increase with an increase in the particle size of the powders. The microhardness and oxygen content of coatings decrease with an increase in the particle size. However, the size of silicon particles has little impact on the deposition efficiency of silicon under the same deposition conditions.

Keywords: Plasma spraying; Silicon coatings; Particle characteristics; Oxidation; Microstructure

1. Introduction

Plasma spraying technology has intensive applications in industrial fields, due to its advantages such as high deposition rate, low cost, and ability to cover large area. During the spraying process, powder particles are injected into the hot gas stream where they are heated, melted and simultaneously accelerated, then finally deposited on the surface of substrates. The coating is built up by the successive deposition of lamellae issued from the solidification of impinging molten particles and the packing of many individual lamellae constitutes the coating. For a given system, the substrate temperature (or its thermal history) plays a relevant role in determining the microstructure of the coatings [1,2]. However, the main factors that control the coating microstructure are velocity, temperature and particle size distribution of the spray droplets at impact [3]. The microstructure of coatings has great influence on their properties and warrants the needed properties of coatings. Better understanding of the phenomena occurring in spraying process is beneficial for the improvement of the quality of coatings. Therefore, the analysis of particle behaviors within the spray jet has been carefully studied by the implementation of on-line monitoring systems [4–6].

Silicon coatings fabricated by plasma spraying technology have been already developed and their performances have been studied for many years. Suryanarayanan et al. [7–9] studied the electrical properties of plasma sprayed silicon coatings. Tamura et al. [10] fabricated solar cells using plasma sprayed silicon coatings and obtained a photoelectric transformation efficiency of 4.3%. Kharas et al. [11] examined the electrical resistivity of the as-deposited and heat-treated silicon coatings and indicated that thick silicon coatings (typically 10–1000 μm thick) deposited by plasma spraying would enlarge the applications of silicon material in meso-scale or direct-write electronics. Silicon coatings were also considered to be used as protective coatings for graphite and metal substrates [12,13]. Silicon has low melting temperature (1420 °C) and is easy to be oxidized in environment containing oxygen. The phenomenon of oxidation

* Corresponding authors at: Shanghai Institute of Ceramics, Chinese Academy of Sciences, 1295 Dingxi Road, Shanghai 200050, China.
Tel.: +86 21 52414103; fax: +86 21 52414104.
E-mail addresses: yrniu@mail.sic.ac.cn (Y. Niu), xbzheng@mail.sic.ac.cn (X. Zheng).

0272-8842/$36.00
http://dx.doi.org/10.1016/j.ceramint.2012.03.080

significantly influences the phase composition, microstructure and properties of the as-sprayed coatings. Therefore plasma sprayed silicon coatings exhibited a complex microstructure and chemical composition [11,14,15]. Akani et al. [16] deposited silicon coatings using air plasma spraying technique and paid attention to the influence of spraying process parameters on the electrical properties (mainly resistivity and mobility) of the coatings. However, they ignored the oxidation phenomenon of silicon powders during spraying and its influence on the electrical properties of silicon coatings. The previous works in our laboratory have reported the phase composition and microstructure characteristics of silicon coating prepared by air plasma spraying [14].

In the present work, silicon powders with different particle sizes (medium size of 114 μm, 79 μm and 31 μm, respectively) were applied to fabricating silicon coatings by air plasma spraying technology. The characteristics of the as-received and in-flight particles were characterized. The deposition process, microstructure and basic property characters of the silicon coatings were combinedly studied. The oxidation phenomenon of silicon particles during fabricating process and its influence on the microstructure and properties of the resulted coatings were emphasized. The aim of this work is to give more information about plasma sprayed silicon coatings, which is beneficial for understanding their special characters and expanding the fields of applications.

2. Experimental procedures

2.1. Particle characterization

Three types of commercially available silicon powders (Nan'an Sanjing Silicon Refining CO., Ltd., China) were used as the starting particles. The silicon powders have a purity of 99.9%, which is measured using chemical method and afforded by the manufacturer. Their particle size distributions and specific surface areas were measured by laser diffraction in wet mode using a BT-9300S system (Baite Instruments Ltd., China). The morphologies of as-received and plasma processed silicon particles were observed using a scanning electron microscopy (SEM, EPMA-8705QH, Shimadzu, Japan).

2.2. Preparation of silicon coatings

The coating specimens were deposited with a Metco A-2000 atmospheric plasma spraying equipment (Sulzer Metco, F4-MB gun, Switzerland). Argon and hydrogen were used as the plasma forming gases. The Twin-System (Plasma-Technick, Switzerland) was used for powder feeding. Titanium alloy plates (Ti–6Al–4V) with dimensions of $10 \times 10 \times 2$ mm^3 were used as substrates, which were grit-blasted with alumina abrasive and cleaned with acetone before plasma spraying process. The mean roughness (Ra), peak-to-valley roughness (Rz) and maximum roughness (Rmax) of the substrate after grit-blasting are 7.55 μm, 43.43 μm and 57.53 μm, respectively. The applied plasma spray parameters are listed in Table 1. A free-standing coating specimen with thickness of about 2 mm was also deposited on a water-cooled aluminum alloy substrate and then was removed from the substrate. The samples for TEM observation and characterization of properties were cut from the free-standing coating using a low-speed diamond wheel saw cutoff machine.

Table 1
Summary of the operating deposition parameters.

Parameters	Values	Units
Power	32	kW
Sprayed distance	120	mm
Primary gas (Ar)	42	slpm[a]
Second gas (H_2)	8	slpm
Powder feed rate	10	g min^{-1}
Carried gas (Ar)	4.5	slpm
Anode internal diameter	7.0	mm
Spray velocity	8	mm s^{-1}
Substrate temperature	25	°C

[a] Standard liters per minute.

2.3. In-flight particle measurement

The temperature and velocity of the melted particles in plasma jet were measured by an on-line monitoring system (Spraywatch2i, Oseir, Finland). The system is based on a digital CCD camera and specially resolving optics. The optics, together with the camera controlled by a computer and a dedicated image processing software enables the on-line measurement of the velocity and temperature of in-flight particles. The details about the diagnostic procedure of in-flight particles are presented in the previous study [17]. The position of the detection was 120 mm downstream from the plasma gun nozzle, where the particles impacted on the substrate. It should be pointed out that this device allows measuring only emissive particles: unmolten ones are not detected. To get a deeper understanding about the formation of microstructures of coatings, single splats were also examined to observe the melted states of powders in plasma flame. For this purpose, the plasma processed silicon particles were collected on unheated glass substrates.

2.4. Characterizations of silicon coatings

The phase composition of the as-sprayed coating was examined by X-ray diffractometry (XRD, RAX-10 X-ray diffractometer, Rigaku, Japan) operating with Cu Kα (λ = 1.54056 Å) radiation. The scanning step of XRD analysis is 0.02° with a fixed counting time of 1 s. The surface morphologies and cross-sectional microstructures of the coatings were observed by SEM. The microstructure of the coating was characterized with a transmission electron microscopy (TEM, JEM-200CX, JEOL, Japan).

The characteristics of surface roughness of the coatings (Ra, Rz and Rmax) were measured by a profilometer (Hommelwerke T8000-C, Germany), which were measured on 3 samples with 5 measurements for each one. The average void content of the coatings was determined by 5 cross-sectional images with a

magnification of 1000× and a resolution of 270 ppi, using an image software (Leica Qwin, Germany). The content of oxygen was also examined by an oxygen–nitrogen analytical instrument (TC-600C, Leco, USA). The deposition efficiency was calculated from the coating mass and the corresponding feedstock mass delivered to the torch. The former was directly measured using a balance with a resolution of 0.01 g and the latter was determined from the powder feed rate and the spraying time on the substrate. Three measurements were performed to determine the oxygen content and deposition efficiency for each coating. The microhardness of silicon coatings was examined using a microhardness instrument (HX-1000, China) under a load of 0.49 N with a dwell time of 15 s. The hardness values represent the average of 20 single measurements.

3. Results and discussion

3.1. Silicon particle characteristics

The size distributions of the three different silicon powders are displayed in Fig. 1. It can be seen that the medium size (D_{50}) of three kinds of powders was 114 μm, 79 μm and 31 μm (denoted as P1, P2, P3), respectively. Three points of distribution D_{10}, D_{50} and D_{90} of these powders and their specific surface areas are summarized in Table 2. The shape of the powders was similar and irregular, as the inserts illustrated.

Table 2
Characteristics of the powders obtained from particle size distributions.

Powder	D_{10} (μm)	D_{50} (μm)	D_{90} (μm)	Specific surface area (m^2/kg)
P1	34	114	241	33
P2	23	79	172	46
P3	9	31	68	116

Fig. 2 presents the measured temperature and velocity variation for the three powders in plasma jet at a stand-off distance of 120 mm versus time. It shows that the temperature and velocity of silicon particles in the plasma flame are greatly influenced by the particle size of the as-received powders. The average temperature (denoted as AT) and average velocity (denoted as AV) of P1, P2 and P3 powders were then calculated based on the measured values in Fig 2a and b, respectively. The

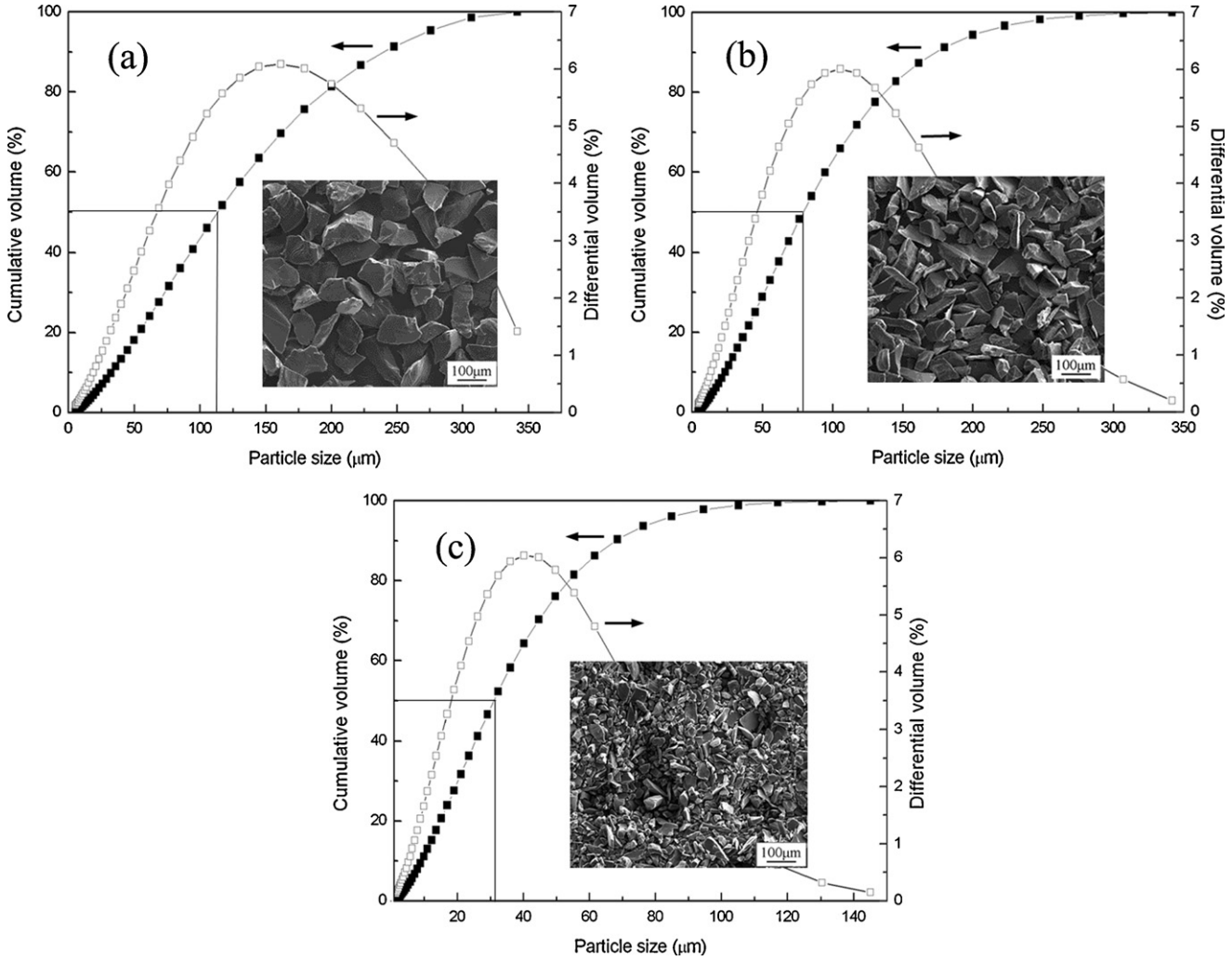

Fig. 1. Particle size distributions and morphologies of three kinds of silicon powders: (a) P1; (b) P2; (c) P3.

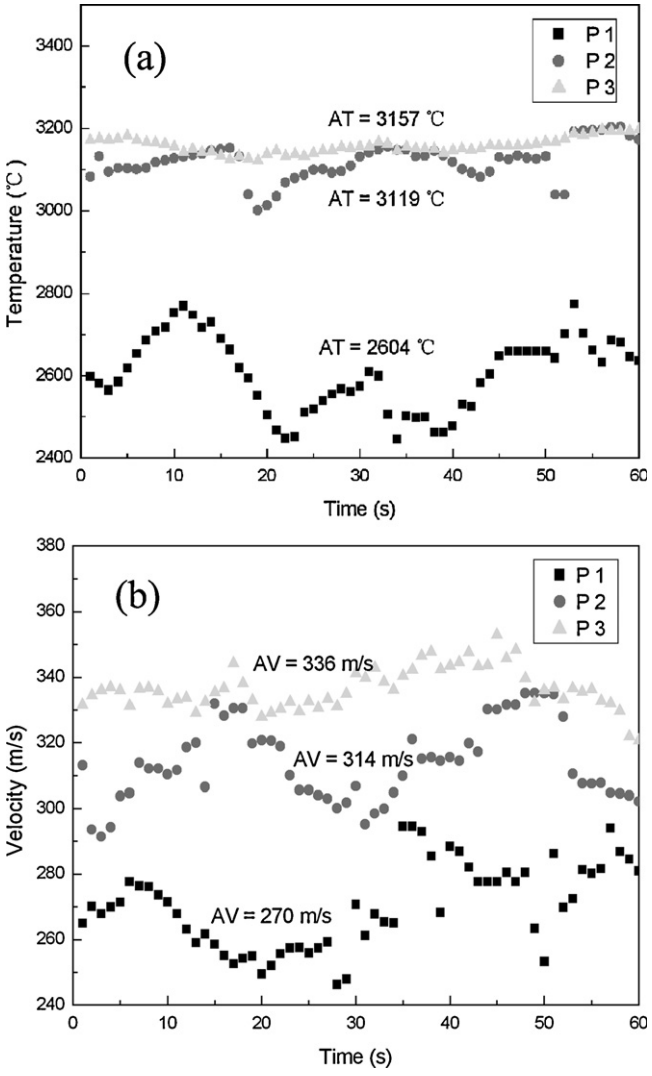

Fig. 2. Temperature (a) and velocity (b) variations with time of silicon particles in plasma flame.

AT of P1, P2 and P3 powders is 2604 ± 90 °C, 3119 ± 45 °C and 3157 ± 19 °C, respectively. The AV of P1, P2 and P3 powders is 270 ± 13 m/s, 314 ± 11 m/s and 336 ± 6 m/s, respectively. It can be seen that the temperature and velocity of in-flight powders decrease with increasing the particle size. The heat and momentum transferred from the plasma gas to the particles have great dependence on the mass and volume of the injected particles [18,19]. Due to the smallest heat capacity and volume, P3 powder exhibited the highest in-flight temperature and velocity among the three types of powders.

The morphologies of melted silicon particles collected on glass substrates are shown in Fig. 3. It is observed that the splat diameter of most of the spread P1 particles was larger than 100 μm (Fig. 3a). Some lamellae of P2 powders distributed on the substrate surface were of diameter less than 100 μm. It is worth noticing that there was a rough villous film covering the surface of glasses substrate (Fig. 3b). For P3 powder, the lamellae exhibited smaller equivalent diameters and also formed a villous film (Fig. 3c). The content of the formed villous film was higher with P3 powder compared to P2 one. From the high magnification, it can be seen that the formed film was of loose microstructure.

The melting and boiling points of silicon material are 1693 K and 2628 K, respectively. Its vapor pressure increases with an increase in the temperature, as illustrated in Fig. 4. It can be seen that the vapor pressure of silicon is about 1×10^3 Pa at its boiling point and is higher than 1×10^5 Pa at 3000 K. The vaporization of silicon becomes significant when the temperature increases. Pfender et al. [20,21] have already convinced the phenomena of air entrainment during atmospheric spraying. It is supposed that the vaporized silicon reacted with the entrapped or surrounding air and formed silicon oxide dust during the spray process, which then condensed on the surface of pre-deposited coatings forming the rough film. The phenomena of vaporization and oxidation are more serious for small particles which have higher surface-to-volume ratios and higher surface temperature. Therefore, the content of silicon oxide is high for P3 powder.

3.2. Microstructure of the coatings

The silicon coatings deposited using P1, P2 and P3 powders are denoted as C1, C2 and C3, respectively. The XRD patterns of C1, C2 and C3 coatings are displayed in Fig. 5. It shows that only the diffraction peaks corresponding to cubic silicon emerged and no silicon oxide was detected in all of the silicon coatings. The observation of silicon splats convinced that silicon oxide formed in the spraying process. It is supposed that the amount of the formed silicon oxide is below the detection limit (5%) of XRD, contributing to this phenomenon.

The surface morphologies of the silicon coatings at low and high magnifications are presented in Fig. 6. All coatings exhibited rough surface, which is the characteristic of plasma sprayed coatings. The surface roughness values (Ra, Rz and Rmax) of the coatings are compared in Table 3. It can be seen that C3 coating has the smallest surface roughness. The feedstock particles of larger size results in the formation of rougher coating surface, which is in accordance with the works of Reisel [23]. It is interesting that there were many small ball-like particles with micrometer sizes on the coating surface. The small particles were splash debris from the impacting silicon splats due to their low viscosity, which were also observed in vacuum plasma sprayed silicon coatings [24]. From the high magnification of the C3 coating (Fig. 6f), it obviously can be seen that there was a villous film covering the surface of C3 coating. The villous film on the coating surface is similar to that observed for the splats, which is supposed to be resulted from the volatilization and oxidation of melted silicon particles during the spraying process and their recondensation after the deposition. Fig. 7 gives the cross-sectional morphologies of C1, C2, and C3 coatings. It can be seen that most of the voids distributed in the three silicon coatings are less than 5 μm in diameters. Some large voids of diameter near 10 μm also existed. For all the coatings, no apparent delaminations were found inside or at their interfaces between the coatings and substrate.

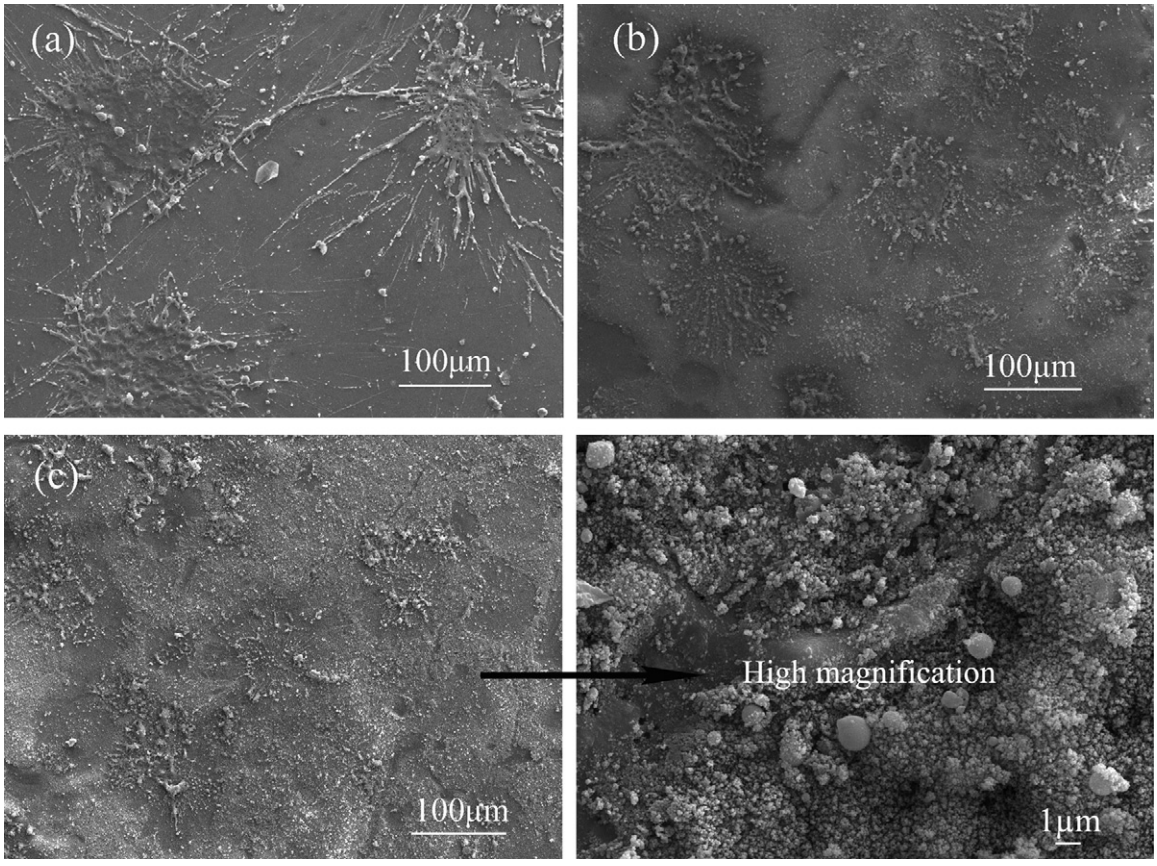

Fig. 3. Morphologies of the splats of silicon powders: (a) P1; (b) P2; (c) P3.

The C3 coating sample was chosen for TEM observation to further explore the microstructure character of air plasma sprayed silicon coatings. Fig. 8 presents the TEM image of the longitudinal section of C3 coating, which is parallel to the spraying direction. It can be seen that the flattened splats overlapped each other, forming a lamellar structure. Both close contact and obvious departing interfaces between splats were found and some voids can be detected at the interfaces, as the arrows pointed at. It is supposed that the molten silicon particles traveled through air and their surface was readily oxidized. The preserved silicon oxide contributed to the formation of interfaces and micropores. A typical oxidized area of the coating is displayed in Fig. 9. The results of EDS prove that the black area is composed of silicon and the gray area of silicon oxide. The SAD pattern indicates that silicon oxide is amorphous. The silicon oxide was surrounded by silicon

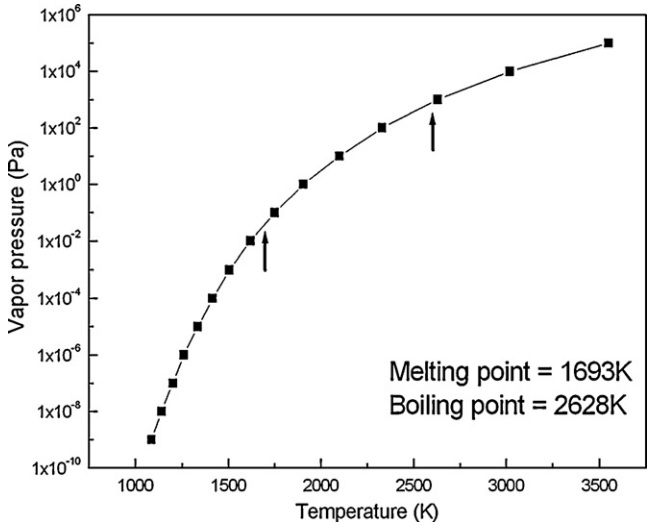

Fig. 4. Vapor pressure of silicon at different temperatures [22].

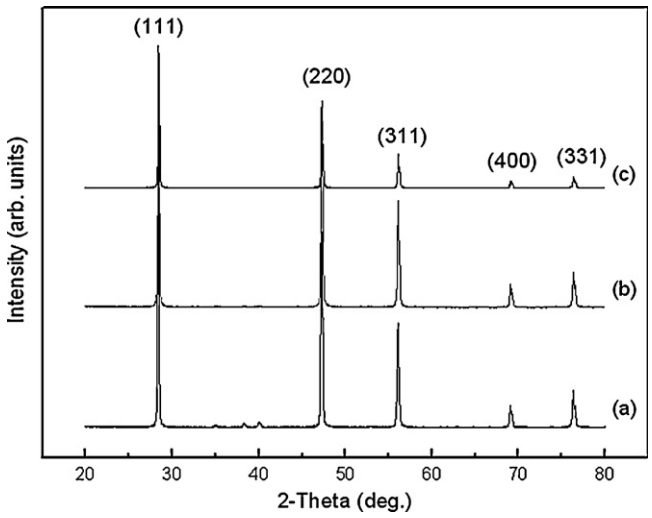

Fig. 5. XRD patterns of silicon coatings: (a) C1; (b) C2; (c) C3.

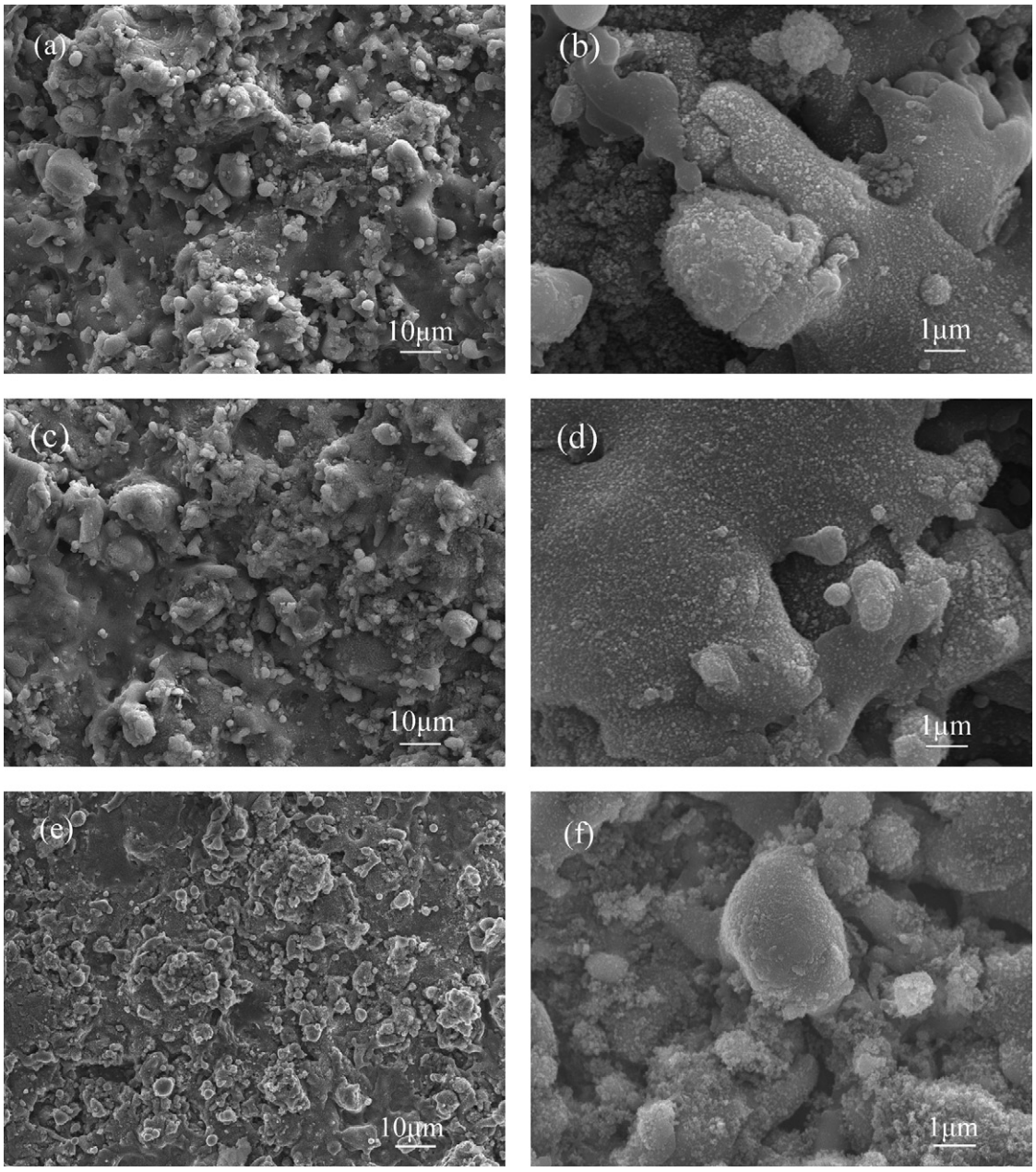

Fig. 6. Surface morphologies of silicon coatings: (a and b) C1; (c and d) C2; (e and f) C3.

particles with ball-like shape. The TEM observation corresponding to the area of small ball-like particles gathered was also observed in the fracture section of silicon coatings, as described in our previous works [25]. The combined results indicate that there are many areas of silicon oxide in the micrometer size range randomly distributing in air plasma sprayed silicon coatings.

Table 3
Surface roughness comparison of silicon coatings.

	C1	C2	C3
Ra (μm)	6.51 ± 0.77	5.24 ± 0.53	3.86 ± 0.44
Rz (μm)	35.85 ± 3.51	30.16 ± 3.52	22.75 ± 1.95
Rmax (μm)	45.63 ± 5.86	36.24 ± 4.03	28.80 ± 5.32

3.3. Characteristics of the coatings

The influence of powder size on some characteristics of silicon coatings, including oxygen content, void content, microhardness and deposition efficiency, was also evaluated. Results are displayed and summarized in Table 4.

The average oxygen contents of C1, C2 and C3 coatings are 0.64 wt%, 0.82 wt% and 1.19 wt%, respectively. The oxygen content of the coating increases with a decrease in the particle size. Oxidation and evaporation phenomena of silicon particles during spraying process have been confirmed by the observation of melted silicon particles. It indicates that the oxidation and evaporation phenomena are much higher for small particles with larger specific surface area and higher surface temperature. Combined with the SEM observations and oxygen content

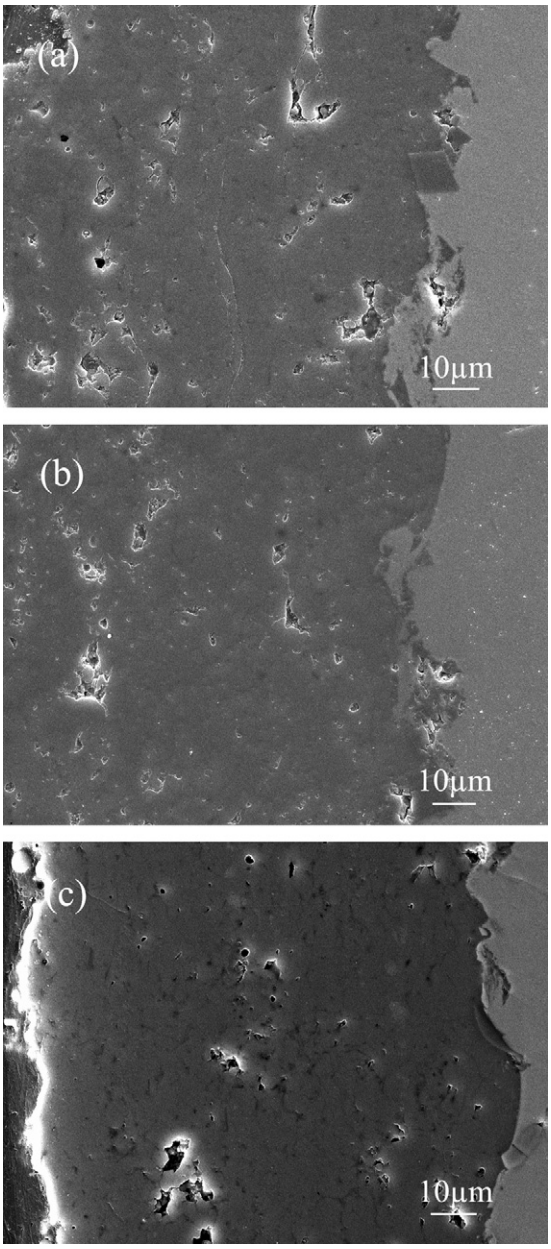

Fig. 7. Cross-sectional micrographs of silicon coatings: (a) C1; (b) C2; (c) C3.

measurements, it can be concluded that the particle size of as-received powders has substantial effect on the oxygen content in silicon coatings. Li et al. [26] studied the effect of particle size of the sprayed powders on the oxidation behavior of MCrAlY coatings fabricated by high velocity oxygen-fuel spraying and found a similar phenomenon.

The average void contents of the as-sprayed C1, C2 and C3 coatings are 11.7%, 10.2% and 8.1%, respectively. The average microhardness of C1, C2 and C3 coatings is 4.00 GPa, 4.36 GPa and 4.99 GPa, respectively. It indicates that the void content of the coating increases with the increase of particle size and the microhardness decreases with increasing particle size. The plasma sprayed coatings are built up by melted particles. Smaller particles had higher impact temperature and velocity on the substrate, as confirmed by the on-line

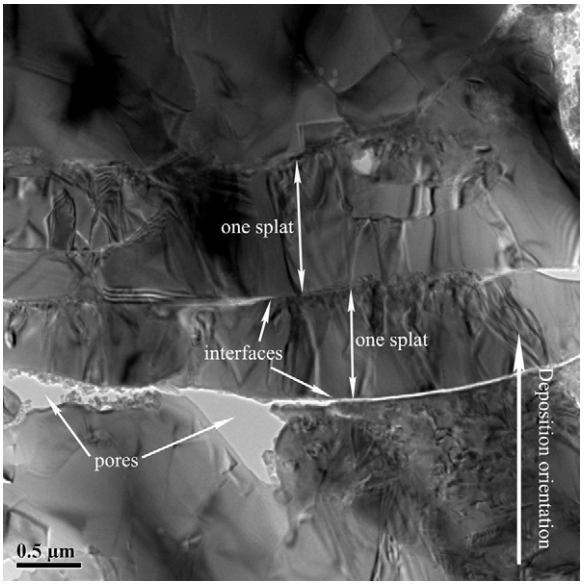

Fig. 8. TEM micrograph obtained from longitudinal section of silicon coating.

measurement. The faster molten particles deform more readily on impact, which increases the resulted coatings' coherence and reduces its void content. Therefore, C3 coating has the highest microhardness among the three coatings, though its content of silicon oxide is high.

It is interesting to find that three kinds of silicon coatings have similar deposition efficiencies under the same operating parameters, indicating that the particle size has little effect on the deposition efficiency values. Deposition efficiency is regarded as being closely related to the melting state of the as-received powders [27]. The measured temperatures of the three kinds of in-flight silicon particles are all much higher than the melting point of silicon (Fig. 2a). However, it should be pointed out that the measured temperature value is the surface temperature of melted particles and not un-melted ones. As well known, high temperature and velocity gradients exist in the plasma flame. Though the thermal conductivity of silicon is high, the retention time of particles in the plasma flame is limited. It is supposed that temperature gradient inside particles also exists, especially for the particles with large size. Therefore, some semi-melted particles existed and were collided and flashed from the substrate, which resulted in the low deposition efficiency for the large silicon particles. For the small particles, the temperature gradient in the particle is little. However, their oxidation and evaporation phenomena in the deposition process were serious, contributing to the low deposition rate.

Table 4
Property characteristics of silicon coatings.

	C1	C2	C3
Oxygen content (wt%)	0.64 ± 0.06	0.82 ± 0.08	1.19 ± 0.11
Void content (%)	11.7 ± 2.2	10.2 ± 1.5	8.1 ± 1.3
Microhardness (GPa, 0.49 loading)	4.00 ± 0.50	4.36 ± 0.41	4.99 ± 0.52
Deposition efficiency (%)	19.0 ± 1.8	20.0 ± 2.0	19.8 ± 1.2

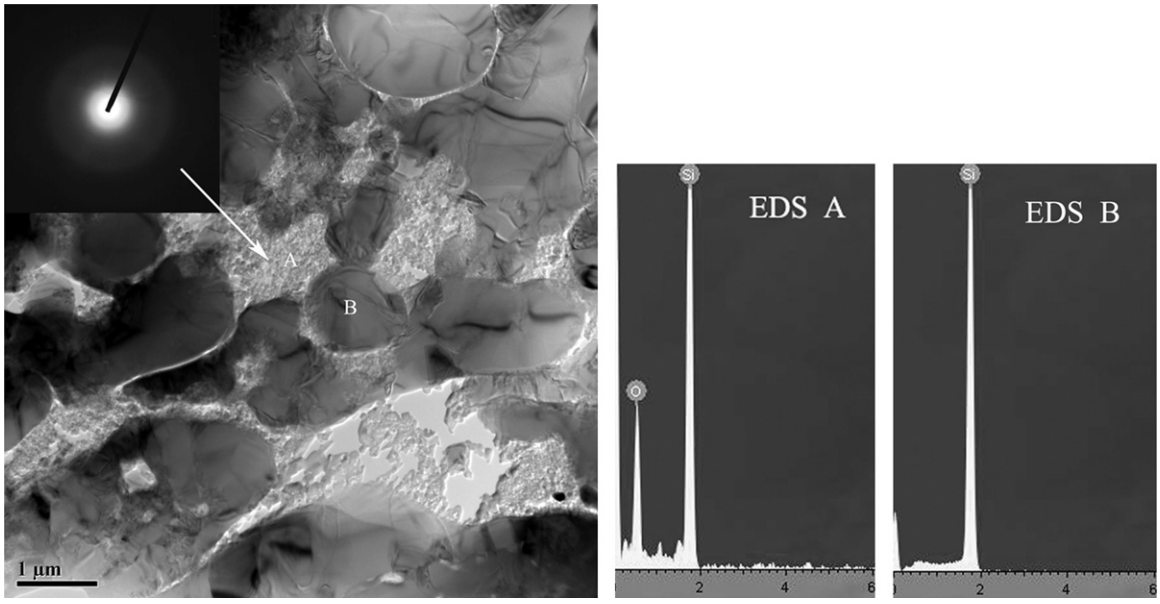

Fig. 9. TEM morphology of a selected area of silicon coating and corresponding electron diffraction pattern and EDS spectra.

4. Conclusions

Plasma sprayed silicon coatings were deposited using silicon powders with three medium sizes. The characteristics of silicon particles before spraying and in plasma flame were analyzed and their influence on the microstructure and properties of resultant coatings was explored. The results showed that the velocity and temperature of in-flight particles increased with decreasing the particle size. The splat-morphologies of different particles were similar, while the oxidation of silicon splats is emphasized for smaller particles. Encapsulated areas of silicon oxide are randomly distributed in the coating. The silicon coatings fabricated with the smallest powder particles had the maximum oxygen content and microhardness, while having the minimum surface roughness and void content. The deposition efficiencies for the three silicon coatings were similar, which was supposed to be resulted from the combined functions of evaporation, oxidation and sputtering of silicon particles during spraying process. These results might be inspiring for fabrication of non-oxide coatings by plasma spraying technology.

References

[1] X. Jiang, J. Matejicek, S. Sampath, Substrate temperature effects on the splat formation, microstructure development and properties of plasma sprayed coatings. Part II. Case study for molybdenum, Materials Science and Engineering A 272 (1999) 189–198.
[2] S.C. Wu, H.O. Zhang, Q. Tang, L. Chen, G.L. Wang, Meshless analysis of the substrate temperature in plasma spraying process, International Journal of Thermal Science 48 (2009) 674–681.
[3] H.D. Steffens, Metallurgical changes in the arc spraying of steel, British Welding Journal 13 (1994) 597–605.
[4] L. Zhao, M.M. Maurer, F. Fischer, E. Lugscheider, Study of HVOF spraying WC-CoCr using on-line particle monitoring, Surface and Coatings Technology 185 (2004) 160–165.
[5] Z. Yin, S. Tao, X. Zhou, C. Ding, Particle in-flight behaviors and its influence on the microstructure and mechanical properties of plasma-sprayed Al_2O_3 coatings, Journal of the European Ceramic Society 28 (2008) 1143–1148.
[6] M.P. Planche, H. Liao, C. Coddet, Relationships between in-flight particle characteristics and coating microstructure with a twin wire arc spray process and different working conditions, Surface and Coatings Technology 182 (2004) 215–226.
[7] R. Suryanarayanan, G. Brun, M. Akani, Growth and electrical properties of plasma-sprayed silicon, Thin Solid Films 119 (1984) 67–73.
[8] B. Kayali, M. Rodot, R. Suryanarayanan, L. Quangnam, R. Mghaieth, R. Gauthier, P. Pinard, High electron diffusion length silicon ribbons by plasma torch projection, Materials Science and Engineering B 5 (1989) 51–56.
[9] M. Akani, R. Suryanarayanan, G. Brun, Resistivity, photoconductivity of plasma-sprayed polycrystalline silicon, Thin Solid Films 151 (1987) 343–353.
[10] F. Tamura, Y. Okayasu, K. Kumagai, Fabrication of poly-crystalline silicon films using plasma spray method, Solar Energy Materials and Solar Cells 34 (1994) 263–270.
[11] B.D. Kharas, G. Wei, S. Sampath, H. Zhang, Morphology and microstructure of thermal plasma sprayed silicon splats and coatings, Surface and Coatings Technology 201 (2006) 1454–1463.
[12] D.J. Varacalle, H. Herman Jr., G.A. Bancke, T.D. Burchell, G.R. Romanoski, Vacuum-plasma-sprayed silicon coatings, Surface and Coatings Technology 49 (1991) 24–30.
[13] A. Ohmori, Z. Zhou, C.J. Li, Characterization of graded Ti silicide coating formed by thermal diffusion treatment of low pressure plasma sprayed silicon coating, in: Proc. 15th Int. Thermal Spray Conf., Nice, France, 1998.
[14] Y. Niu, X. Liu, C. Ding, Phase composition and microstructure of silicon coatings deposited by air plasma spraying, Surface and Coatings Technology 201 (2006) 1660–1665.
[15] H. Fujishiro, S. Furukawa, I. Takahashi, T. Kuwashima, Structure and electrical properties of low-pressure-plasma-sprayed silicon-based materials, Journal of the Ceramic Society of Japan 102 (1994) 1–4.
[16] M. Akani, R. Suryanarayanan, G. Brun, Influence of process parameters on the electrical properties of plasma-sprayed silicon, Journal of Applied Physics 60 (1986) 457–459.
[17] Z. Yin, S. Tao, X. Zhou, C. Ding, Particle in-flight behavior and its influence on the microstructure and mechanical properties of plasma-sprayed Al_2O_3 coatings, Journal of the European Ceramic Society 28 (2008) 1143–1148.

[18] R. Westhoff, G. Trapaga, J. Szekely, Plasma-particle interactions in plasma spraying systems, Metallurgical Transactions B 23 (1992) 683–689.
[19] M. Krauss, D. Bergmann, U. Fritsching, K. Bauckhage, In-situ particle temperature, velocity and size measurements in the spray forming process, Materials Science and Engineering A 326 (2002) 154–164.
[20] E. Pfender, Fundamental studies associated with the plasma spray process, Surface and Coatings Technology 34 (1988) 1–14.
[21] R. Spores, E. Pfender, Flow structure of a turbulent thermal plasma jet, Surface and Coatings Technology 37 (1989) 251–270.
[22] R.E. Honig, D.A. Kramer, Vapor pressure data for the solid and liquid elements, RCA Review (1969) 285–305.
[23] G. Reisel, R.B. Heimann, Correlation between surface roughness of plasma-sprayed chromium oxide coatings and powder grain size distribution: a fractal approach, Surface and Coatings Technology 185 (2004) 215–221.
[24] Y. Niu, X. Liu, X. Zheng, H. Ji, C. Ding, Microstructure and properties characterization of silicon coatings prepared by vacuum plasma spraying technology, Journal of Thermal Spray Technology 18 (2009) 427–434.
[25] Y. Niu, X. Liu, Y. Zeng, X. Zheng, H. Ji, C. Ding, Electrical property characterization of plasma sprayed polycrystalline silicon, Materials Science Forum 620–622 (2009) 303–306.
[26] C.J. Li, W.Y. Li, Effect of sprayed powder particle size on the oxidation behavior of MCrAlY materials during high velocity oxygen-fuel deposition, Surface and Coatings Technology 162 (2002) 31–41.
[27] R. Kingswell, K.T. Scott, L.L. Wassell, Optimizing the vacuum plasma spray deposition of metal, ceramic and cermet coatings using designed experiments, Journal of Thermal Spray Technology 2 (1993) 179–186.